# Access of ligands to the ferric center in lipoxygenase-1

Betty J. Gaffney, Dimitrios V. Mavrophilipos, and Kutbuddin S. Doctor
Department of Chemistry, The Johns Hopkins University, Baltimore, Maryland 21218 USA

ABSTRACT A form of ferric lipoxygenase-1 has been isolated that gives an EPR spectrum that is dominated by a species of intermediate rhombicity ($E/D = 0.065$). This species is obtained in the presence of a number of buffers of high concentration and in the absence of fatty acid byproducts of the iron oxidation. The species is unstable over a period of one day with respect to symmetry of the iron. The EPR lineshapes of the unstable species are highly sensitive to the anionic composition of the buffer and to the addition of neutral ligands. These results suggest that newly formed ferric lipoxygenase has weak affinity for a number of ligands. Affinity of charged ligands for the iron center may provide a mechanism for charge compensation as the iron center alternates between ferric and ferrous in the catalytic cycle. We use spectral simulation to evaluate quantitatively the interaction of the ferric center with ligands and also show that a transition in the middle Kramers doublet makes a significant contribution to the EPR spectrum of the more rhombic species.

## INTRODUCTION

In plants and animals, the lipoxygenase family of enzymes catalyzes the conversion of polyunsaturated fatty acids to hydroperoxide derivatives, with regio- and stereochemical specificity (1). In normal cell function, the hydroperoxides are reduced to hydroxy fatty acids (2) or undergo enzymatic conversion to important metabolites including lipoxins and leukotrienes (3). In pathological conditions, for instance in atherosclerosis (4, 5), lipoxygenase activity may result in formation of free radical by-products (6). The structure (7–10) and mechanism (11) of lipoxygenases are subjects of current study. Many of the mechanistic questions to which answers are being sought center around the role of a mononuclear iron in the normal chemistry of the lipoxygenases and in the abnormal production of free radicals.

Electron paramagnetic resonance spectroscopy (EPR) has already provided key information about the role of the iron atom in the mechanism of lipoxygenases: a high-spin ferric form of the enzyme undergoes anaerobic reduction by the substrate. The high-spin ferric form, itself, results from oxidation of a high-spin ferrous, resting form of the enzyme (12–14). On these bases, the catalytic cycle is thought to involve both ferric and ferrous forms of the enzyme (11). Most previous EPR experiments have been carried out on lipoxygenase-1 (L-1), the major lipoxygenase isozyme from soybeans. Recent papers have shown that the iron center in other lipoxygenases gives EPR spectra under conditions similar to those used with L-1 (15). The EPR spectra of ferric lipoxygenases might be used in further studies to obtain information about the nature of the iron ligands, by ENDOR or ESEEM, or about formation of kinetic intermediates. These goals are complicated, however, by the existence of multiple, overlapping EPR spectra. Previous studies have shown that a single-component EPR spectrum can be obtained by adding ethanol to a lipoxygenase sample with a multi-component EPR spectrum and that cyanide, SDS and salt alter the ratios of components that make up the spectrum (16). Here we describe experiments showing that a species giving rise to the other major component of the multi-component EPR spectrum is obtained when ferric lipoxygenase is prepared in the presence of some buffer anions and neutral ligands. Isolation of this species is important in two ways: (*a*) we find that there are time-dependent changes in the symmetry of the L-1 iron center after it has been oxidized to the ferric form and (*b*) we are able to improve simulations (17) of the ferric L-1 lineshapes. We use spectral simulation to evaluate the interaction of the ferric center with ligands and also show that a transition in the middle Kramers doublet makes a significant contribution to the spectrum of the more rhombic species.

Multi-component EPR spectra arising from several different symmetries at the metal center are a common feature of EPR spectroscopy of ferric proteins. The nonheme ferric forms of transferrin (18), iron superoxide dismutase (19) and phenylalanine hydroxylase (18) exhibit multi-component spectra and catalase is an example of a heme enzyme with multiple EPR spectra (20). Computer simulation is often required to determine the number and proportions of spectral components displayed by an EPR sample (21, 22). We present simulations showing that the EPR spectra of lipoxygenase-1 are composed, in most cases, of sub-spectra from at least 2 species. An earlier simulation of the EPR spectra of L-1 used angle dependent linewidths to achieve a reasonable fit to experimental spectra (17). We have been able to account for this linewidth variation, instead, in terms of distributions of energy separations for the six-level $S = {}^5/_2$ state. Our computer program for lineshape simulation has been discussed in a recent review (22). An earlier program was used in simulations of the multi-component EPR spectra of ferric transferrin and phenylalanine hydroxylase (18).

## METHODS

All anionic buffers used are sodium salts. Buffers for lipoxygenase purification are designated buffer A (0.02 M phosphate, pH 6.8) and buffer B (0.2 M phosphate, pH 6.8).

Address correspondence to Betty J. Gaffney, Department of Chemistry, The Johns Hopkins University, 3400 Charles St., Baltimore, MD 21218.

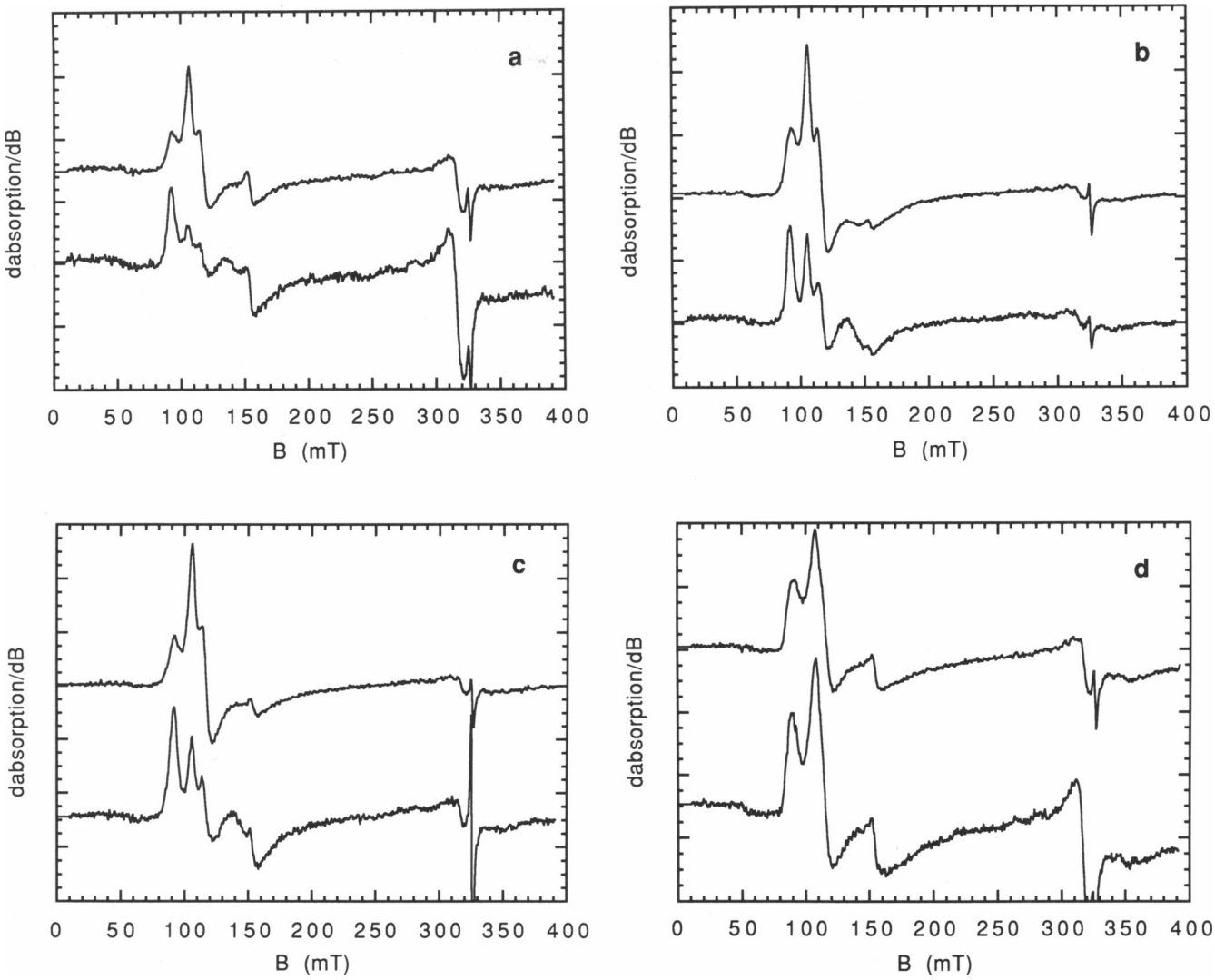


FIGURE 1 Electron paramagnetic resonance spectra are shown for lipoxygenase samples which have been converted to the ferric form by oxidation with one equivalent of the 13-hydroperoxide derivative of linoleic acid (13-HPOD) at various pH's and ionic strengths. Fatty acid byproducts of the oxidation were not removed from the samples used for this figure. In each panel, the upper spectrum is from 70 $\mu$M ferric lipoxygenase-1 (L-1) in 5 mM buffer; the lower spectrum in each panel was from 35 $\mu$M L-1 in 0.1 M buffer. Lower spectra are shown with twice the amplification of the upper ones so that the intensities can be compared directly. Samples at the higher buffer concentration were prepared by adding equal volumes of 70 $\mu$M ferric lipoxygenase in 0.005 M buffer to 0.2 M buffer. Buffers compositions and pH's were (*a*) citrate-phosphate, pH 6.0; (*b*) phosphate, pH 7.0; (*c*) phosphate, pH 8.0; and (*d*) borate, pH 9.0. All spectra were recorded at 4 K with a microwave power of 0.1 mW, modulation amplitude of 20 Gauss and recorder gains of 0.8 to 1.25 $10^{-4}$.

The source of L-1 was usually dried soybeans obtained from a local organic food store. Sigma Chemical Co. (St. Louis, MO) soybean acetone powder or purified soybean lipoxidase (Type V) were purified further in some cases and results reported here are independent of the source of the enzyme. Lipoxygenase-1 (L-1) was partially purified, through the ammonium sulfate precipitation and dialysis steps, following the procedure of Axelrod et al. (23). Further purification of the sample was achieved using two, sequential passes through columns packed with new DE52, anion-exchange resin (Whatman, Hillsboro, OR). For a preparation starting with 500 g of soybeans, the dialysate in buffer A was loaded on the first or second, 100 ml DE-52 column, washed with 2 l of buffer A to remove pigments and other impurities, and eluted with a 1 l gradient from 0 to 0.4 M ammonium sulfate in buffer A. Samples were purified further on a metal-free Dionex (Atlanta, GA) HPLC system equipped with a Dionex ProPac PA1 preparative column (9 × 250 mm) running at 4 ml/min or a Dionex Zorbax® SE-250, size exclusion column running at 3 ml/min. L-1 adsorbs to the ProPac PA1 column in buffer A and is eluted by a variety of 0.2 M solutions. For the Zorbax column, 0.2 M buffers were used. Elution with buffer B, or a gradient from buffer A to B, was used unless otherwise specified. The impurity most difficult to remove during the purification is a yellow-green, low-molecular weight species with $\lambda_{max}$ = 410 nm. It elutes from anion exchange columns slightly after lipoxygenase or is separated by exhaustive dialysis. Activity assays were done with 3 nM L-1 as described (23) with the modification that the assay solution usually contained 40 to 60 units/ml of bovine liver catalase (Sigma C-100). Activities of samples used for EPR were 180 ± 10% $\mu$mol $min^{-1}$ $mg^{-1}$ in the presence of catalase and slightly higher in its absence (24). Iron assays (25) on purified L-1 showed 1 iron per protein. CD spectra at 19°C (200–300 nm) were the same for ferrous L-1 in 0.02 or 0.2 M phosphate buffer at pH 7. The CD spectra appeared identical to those published (26). Freshly prepared L-1 was used for most of the studies reported here. Frozen (−70°C) L-1 samples gradually lose activity, especially when they are stored in low ionic strength buffers.

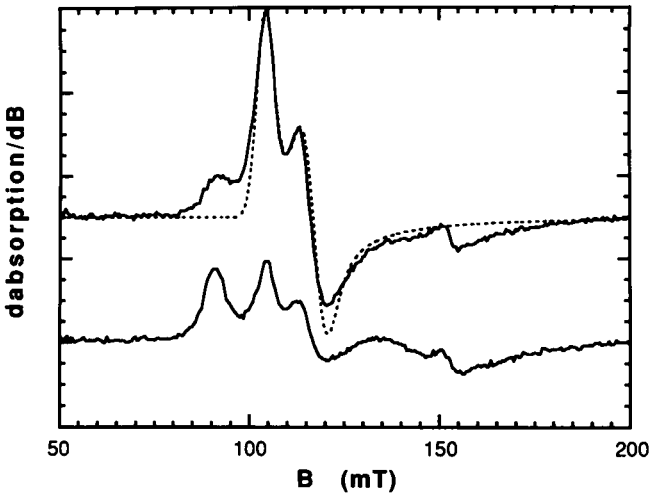


FIGURE 2 The effect of adding glycerol to a sample of freshly-oxidized L-1 is depicted here. The lower spectrum is from a sample prepared as those used for Fig. 1. The buffer is 0.1 M phosphate, pH 7. When glycerol is added to 15% to the sample giving the lower spectrum, the spectrum at the top results. The dashed line is a partial simulation of the more axial component of the spectrum. The simulation parameters are given in Table 2 and are those of axial component II.

As background for studies of variability in the spectra of L-1, EPR spectra were recorded for samples at each stage in the protein purification procedure to determine whether there were impurities that could give significant EPR signals. Spectra of these samples were recorded before and after addition of 1 mM 13-HPOD, the hydroperoxide resulting from oxidation of linoleic acid with L-1. At early stages in the preparation, broad iron signals at $g' = 4.3$ and signals at $g' = 2$ from manganese and copper were visible. As L-1 was purified, these metals signals diminished while signals in the region $g' = 6$ to 8 increased for samples treated with hydroperoxide. Addition of the 13-HPOD to impure samples changed the levels of visible copper or manganese, suggesting that trace metal impurities in lipoxygenase may be capable of catalyzing one electron reactions with fatty acid hydroperoxides.

HPLC purification was used for separation of ferric lipoxygenase from fatty acid byproducts of the activation step. Several different buffers and different pH's were used. Ferrous L-1 was diluted to 1 mg protein/ml in ice-cold, aerated 0.2 M borate buffer at pH 9.2, oxidized by addition of one equivalent of substrate (from a 0.01 M suspension in 0.2 M borate), immediately diluted tenfold with 0.02 M buffer at a lower pH and pumped onto the HPLC column. The column was washed with 100 ml of 0.02 M buffer after elution of material at 234 nm ceased and the ferric protein was eluted with a linear gradient of the sodium salt of the desired anion or by a step from low to high buffer concentration. This procedure was effective for phosphate, carbonate, formate or Tris buffers. The protein could not be eluted from the column with 0.2 M borate, however. Samples eluted from the ProPac PA1 HPLC column had concentrations from 2–6 mg/ml, depending on the portion of the eluted peak retained. There was no detectable difference in elution profiles of ferrous and ferric lipoxygenase when gradient elution was used.

The hydroperoxide product of lipoxygenase action on linoleic acid, used to oxidize resting lipoxygenase in some experiments, was prepared by adding 0.16 mg L-1 to an ice-cold solution of 10 mg of linoleic acid in 200 ml borate buffer, with rapid stirring. After 20 min, the reaction mixture was acidified to pH 3.0, extracted with ether, dried and evaporated. The reaction products were purified preparatively on silica gel TLC using a solvent mixture of toluene:ethyl acetate:ligroin:acetic acid, 100:30:20:1 (vol/vol). HPLC analysis (27) was used to determine the optimum conditions for hydroperoxide formation: more concentrated substrate solutions or longer reaction times gave a number of by-products including the 13-keto- and hydroxy- decomposition products of the desired hydroperoxide. These products were separated from the hydroperoxide by the TLC conditions given above and they exhibited UV spectra (ether) distinct from the hydroperoxide.

Paramagnetic resonance measurements were made on a Varian (Palo Alto, CA) E-109 spectrometer equipped with a reference arm, low power attenuation and an Oxford Instruments (Oxford, N.A., Concord, MA) ESR-9/10, pumped cryostat for liquid helium. Temperatures were usually measured at a thermocouple located below the sample, but in a few experiments, a 4 mm id quartz tube was used in a modified Dewar and a carbon-glass resistance thermometer (Lake Shore Cryotronics, Westerville, OH) was frozen into the top of the sample to calibrate temperatures more accurately. Between 4 and 8 K, the temperature gradient across the sample was less than 0.2 K. The gradient increased as temperatures increased above 8 K. All EPR spectra presented in the figures in this paper were recorded at the base temperature of liquid helium. Data on temperature dependence of saturation used the average of the temperatures above and below the sample. Plots of [intensity/(power)$^{1/2}$] vs. power were made for spectra from samples at 5–25 K. At 5 K the power at which half-saturation ($P_{1/2}$) of EPR features at $g' = 6.1$ occurs is ~2 mW and, at 25 K, it is ~50 mW when 100 kHz field-modulation is used. For the features at $g' = 7.4$, ($P_{1/2}$) at 5 K is 7 mW and, at 25 K, is 85 mW. When protein

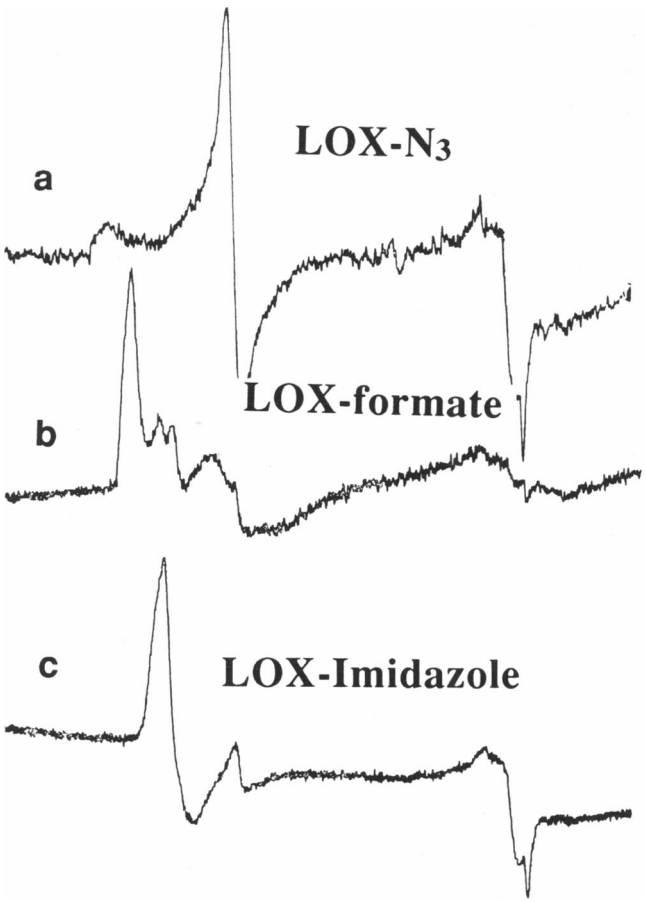


FIGURE 3 EPR spectra of L-1 depend on ligands: (*a*) sodium azide was added to 60 μM lipoxygenase in 0.2 M phosphate, pH 7.0 to a final azide concentration of 0.5 M; (*b*) 60 μM lipoxygenase in 0.2 M formate buffer, pH 7.4 and (*c*) same as *b* except imidazole added to 0.5 M. In each case, ferric L-1 had been separated from fatty acid byproducts by HPLC as described in Materials and Methods.

TABLE 1 **Effect of ligands on lipoxygenase-1 EPR***

| Buffer | pH | Additive | g-value‡ |
|---|---|---|---|
| Phosphate | 6.8 | None | 7.4 |
| Carbonate | 8.0 | None | 7.4 |
| Formate | 6.8 | None | 7.45 |
| | 7.8 | None | 7.45 |
| | 7.0 | 0.05 M pyridine | 7.4 |
| | 7.0 | 0.05 M 3-chloropyridine | 7.4 |
| | 7.0 | 2 mM ethanol | 6.17 |
| | 7.0 | 0.05 M 2-methyl imidazole | 6.2 |
| | 7.0 | 0.05 M imidazole | 6.15 |
| Pyridine (0.1 M)§ | 7.0 | None | 7.4 |
| Pyridine-N-oxide (0.1 M)§ | 7.0 | None | 6.4 |
| 4-picoline (0.1 M)§ | 7.0 | None | 7.4 |
| 4-picoline-N-oxide (0.1 M)§ | 7.0 | None | 6.4 |

* Samples were 1–5 mg/ml in protein. EPR spectra were recorded at 4K.

‡ *g*-Value measured at the first low-field maximum.

§ The EPR spectrum was measured after dialysis for 24 h into the indicated solution with no other buffer. Minor pH adjustments were made with dilute sodium hydroxide or hydrochloric acid.

concentration and temperature permitted, the microwave power used routinely was 0.1 mW. Some signals were recorded, as indicated in the figure legends, at powers up to 1 mW to achieve reasonable signal-to-noise. When 100 kHz modulation is used, large, rapid-passage signals (28) for ferric L-1 can be observed at modest powers (e.g., 5 mW) by recording the second harmonic, in-phase signal. Thus, the apparent $T_2$ for L-1 is probably dominated by the frequency of the 100 kHz field modulation. The EPR signals of some samples were recorded using both 10 and 100 kHz field modulation. Differences between lineshapes recorded under both conditions were extremely small and would not affect conclusions about the relative proportions of the multiple components in the L-1 EPR spectra recorded with the higher modulation frequency.

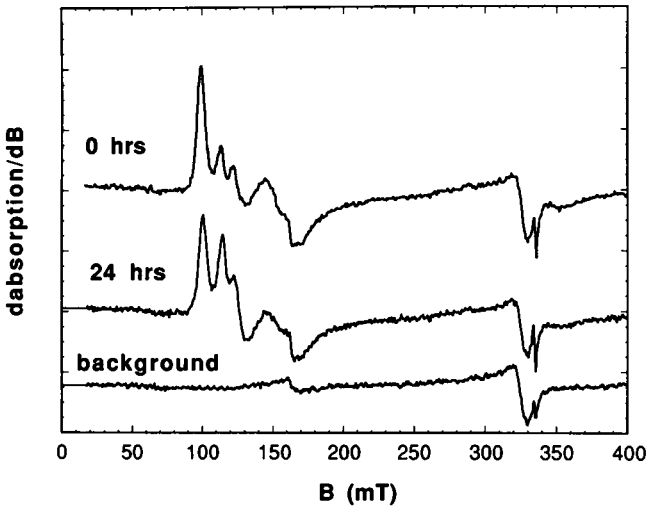


FIGURE 4 The electron paramagnetic resonance (EPR) spectra of lipoxygenase-1 (L-1), prepared by elution from an anion exchange, HPLC column, depend on the length of time the sample is stored at after oxidation to the ferric form. Spectra of samples immediately after preparation and 24 h after preparation are compared with the baseline. The buffer was 0.2 M phosphate, pH 6.8; protein concentration was 60 μM. All spectra were recorded at 4 K with a microwave power of 0.05 mW, modulation amplitude of 10 Gauss and recorder gain of 1.25 $10^{-4}$.

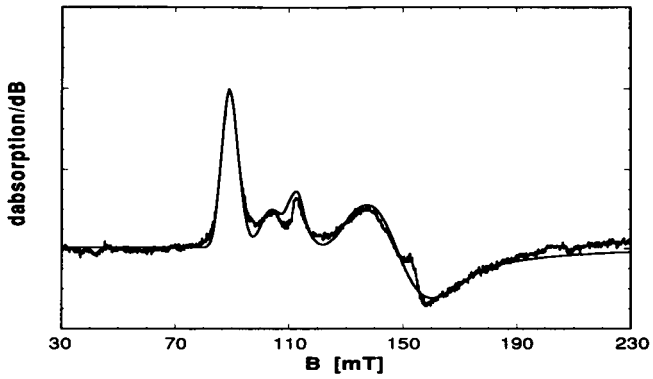


FIGURE 5 The experimental EPR spectrum (noisy line) of an L-1 sample freshly eluted from HPLC in 0.2 M phosphate buffer, pH 6.8, is compared with a computer simulation (*smooth line*) which followed the steps outlined in Fig. 7. Simulation parameters are given in Table 2 with axial component I. The fraction of spins calculated for the minor, near-axial component is 7%.

## RESULTS

It is known that the resting form of lipoxygenase is ferrous and that addition of one equivalent of the hydroperoxy fatty acid derived from linoleic acid (13-HPOD) to the resting form of the enzyme gives a ferric species. We have examined this activation step at different pH's. Fig. 1 shows that the ability of 13-HPOD to oxidize dilute lipoxygenase iron is virtually independent of pH because each sample gives a signal representing the majority of the iron. In this figure, the EPR signals from samples prepared in 0.005 M buffers are shown as the upper spectrum in each panel and the spectra from samples in 0.2 M buffers are shown at the bottom. The signals are particularly dependent on the buffer concentration. The difference in signals between samples in 0.005 M buffers and in 0.2 M ones is most pronounced in the citrate/phosphate buffer at pH 6. Effects of buffer concentration are diminished if L-1 samples have less than maximum specific activity (data not shown). The signals from samples at pH 9.0 in borate buffer are qualitatively different from the others: the apparent linewidths are larger and the position of the low-field maximum is at a slightly higher $g'$ value ($g' = 7.4$ in Fig. 1, *a–c* and 7.45 in Fig. 1 *d*). The changes between 0.005 and 0.2 M buffers are smallest for the borate sample: the ratio of the lowest-field peak to the one next higher in field (more rhombic/near axial) is 0.57 for the sample in 0.005 M borate and 0.67 for that in 0.2 M borate.

Addition of glycerol to the samples in 0.2 M buffer, discussed above, results in an altered EPR spectrum. This result is shown in Fig. 2 for a sample in pH 7 buffer

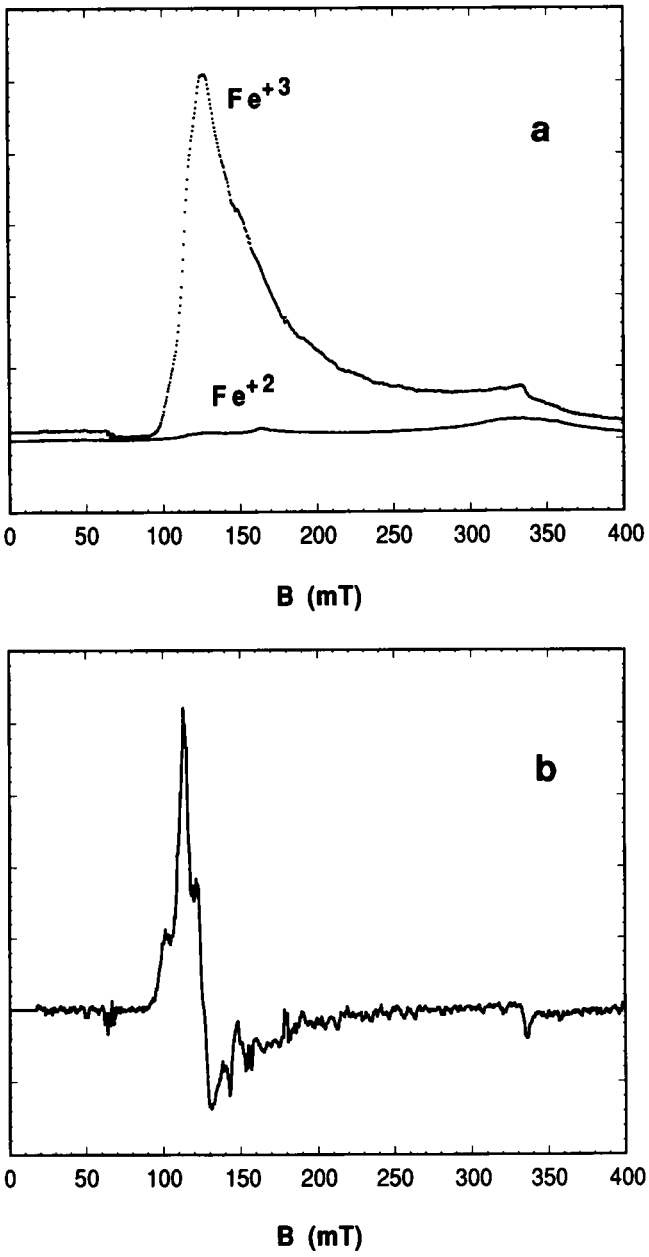


FIGURE 6 Second harmonic spectra of lipoxygenase are recorded under rapid passage conditions. (*a*) In-phase, second harmonic, with respect to 100 kHz modulation, spectra are shown for the ferrous and ferric forms of lipoxygenase. The protein concentration of ferrous protein was 0.6 mM and, and that of the ferric protein was 0.2 mM. The buffer was 0.02 M phosphate, pH 7.0. Instrumental conditions were 5 mW power, 8 G field modulation amplitude and 4 K. Spectra are shown at identical amplifications. (*b*) The smoothed numerical derivative of the ferric second harmonic spectrum shown in *a*.

with (*upper*) and without (*lower*) 15% glycerol. The simulation shown in Fig. 2 (*dashed line*) will be discussed in the next section on spectral simulation.

Since it seems likely that the fatty acid byproducts of the activation step have some affinity for the enzyme, removing them is an important prerequisite to evaluating the EPR spectra. Other investigators have shown that 94% of the products resulting from oxidation of lipoxygenase with U-$^{14}$C-labeled hydroperoxide can be separated from the protein on Sephadex G-25 (16). The Materials and Methods section describes a protocol, using HPLC, that was developed to prepare ferric lipoxygenase in buffers of defined composition and free of fatty acid by-products. The essential features of the protocol are (*a*) oxidation of ferrous lipoxygenase in the presence of a large excess (25-fold) of oxygen to scavenge free radicals, (*b*) separation of fatty acid by-products from ferric lipoxygenase by washing the protein on an anion-exchange, HPLC column with 0.02 M buffer and (*c*) elution of washed, ferric lipoxygenase in the same buffer at 0.2 M. This procedure was effective when the buffer anions were phosphate, carbonate or formate at pH's from 6 to 8. In control experiments using varied mixtures of enzyme and hydroperoxide, fatty acid products from the activation were found to elute with low ionic strength washing with 60–90 ml (depending on pH), while protein was retained on the column. In preparative steps where large volumes of protein solution were loaded on the column, the column was washed with 100 ml of low ionic strength buffer after all of the material absorbing at 234 nm was eluted. In some cases, lipoxygenase was applied to a second HPLC-sizing column to further separate traces of fatty acid from protein.

The protocol described above was employed to evaluate the dependence of the EPR spectra of L-1 on ligands and on time. Fig. 3 shows the effect of bringing fatty acid-free samples, prepared in 0.2 M phosphate or formate, to 0.5 M in azide (*top spectrum*) or imidazole (*bottom spectrum*). The spectrum of L-1 in 0.2 M formate (*middle spectrum*) is almost the same as that for a sample in phosphate (Fig. 1, *b* and *c, lower*) except that the formate samples show evidence of a low-field shoulder corresponding to a component that is slightly more rhombic than the major component in the spectra of samples in 0.2 M phosphate buffer. The effect of azide can also be observed with 0.05 M azide. Table 1 gives a summary of additives that favor the more rhombic ($g'$ = 7–8) or more axial species ($g'$ = 6.1–6.3). Table 1 also includes results of an experiment designed to address whether ligand effects on EPR spectra result from changes in coordination to iron. A number of methyl-

**TABLE 2 Parameters used in simulation of lipoxygenase-1 lineshapes**

| Component | E/D | $\sigma_{E/D}$ | $\sigma_\nu$ |
|---|---|---|---|
| | | | *MHz** |
| Rhombic | 0.065 | 0.011 | 150 |
| Axial-I | 0.0175 | 0.008 | 150 |
| Axial-II | 0.0150 | 0.004 | 150 |

*A linewidth defined for frequency swept spectroscopy ($\Delta\nu$) can be converted to the field-swept linewidth ($\Delta H$) using the following relation: $\Delta\nu$(MHz) × ($h/g'\beta$) = $\Delta H$(Gauss) (18).

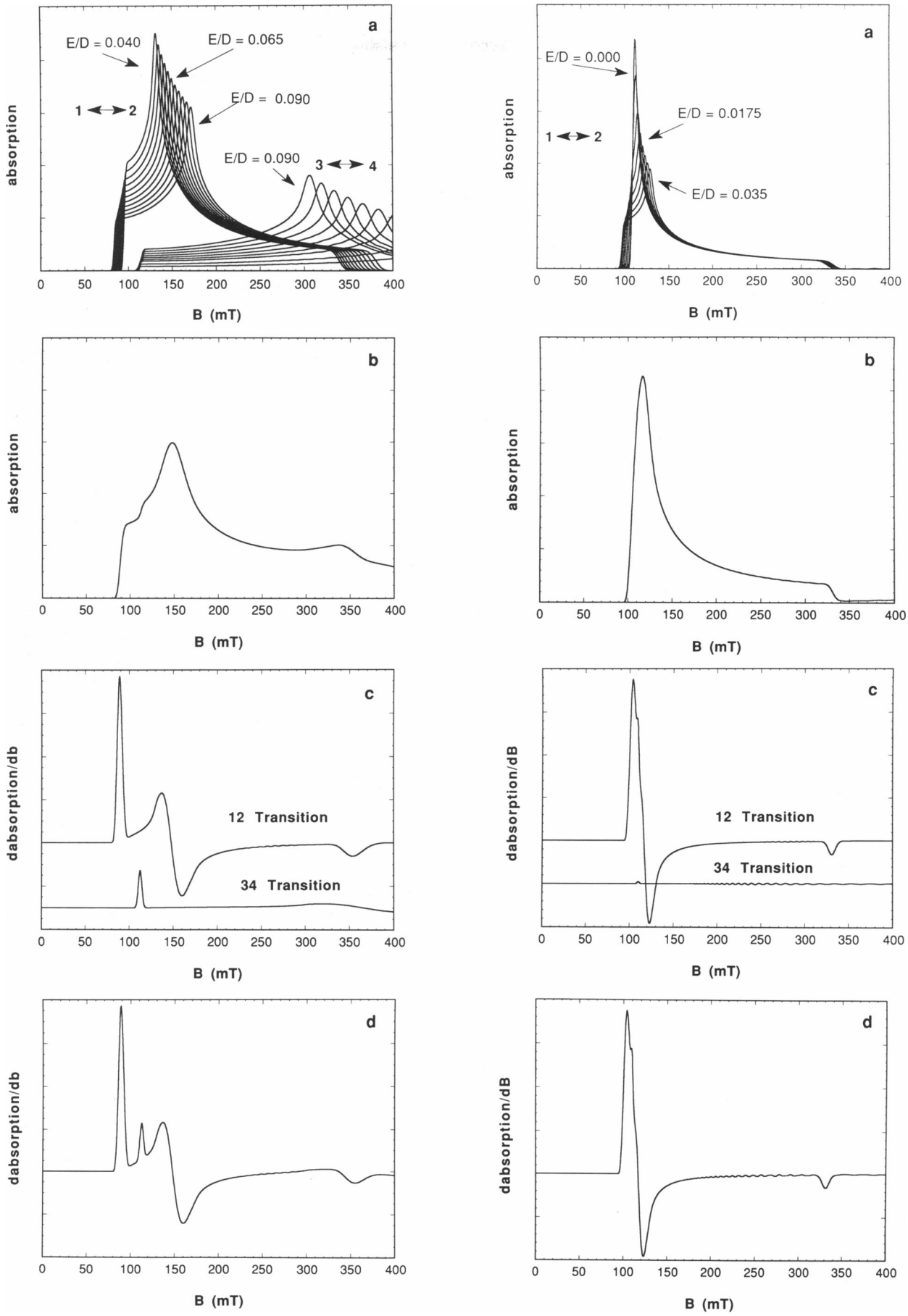
a
E/D = 0.040
E/D = 0.065
E/D = 0.090
1 ↔ 2
E/D = 0.090
3 ↔ 4
absorption
0 50 100 150 200 250 300 350 400
B (mT)
a
E/D = 0.000
E/D = 0.0175
1 ↔ 2
E/D = 0.035
absorption
0 50 100 150 200 250 300 350 400
B (mT)
b
absorption
0 50 100 150 200 250 300 350 400
B (mT)
b
absorption
0 50 100 150 200 250 300 350 400
B (mT)
c
12 Transition
34 Transition
dabsorption/db
0 50 100 150 200 250 300 350 400
B (mT)
c
12 Transition
34 Transition
dabsorption/dB
0 50 100 150 200 250 300 350 400
B (mT)
d
dabsorption/db
0 50 100 150 200 250 300 350 400
B (mT)
d
dabsorption/dB
0 50 100 150 200 250 300 350 400
B (mT)

substituted pyridines (picolines) and their *N*-hydroxy derivatives were tested. The more rhombic species was evident in the EPR spectra of samples containing the picolines while the more axial one was observed for the *N*-hydroxy picolines.

Several experiments were done to examine the stability with time of the species prepared by the HPLC protocol. Fig. 4 shows one example of time-dependent changes in EPR spectra. The spectrum of a sample prepared in 0.2 M phosphate buffer, pH 7.8 as the HPLC eluting buffer is given at the top of Fig. 4 while a spectrum of another portion of the same sample after storage at 10°C for 24 h is given in the middle. The particular sample used for Fig. 4 was passed through a second HPLC size-exclusion column after anion exchange purification on HPLC. This second column was not used routinely. Samples prepared in phosphate or formate buffers were examined for enzyme activity and EPR spectra at intervals over a period of one month. While substantial EPR spectral changes are observed after 24 h, ferric L-1 at pH 7, purified by the anion-exchange HPLC method described above, is usually stable with respect to the standard activity assay for three weeks to one month. After one month, the EPR spectrum has changed further from that shown in the middle of Fig. 4 to one resembling the spectra in Fig. 1 of samples in low-concentration, phosphate buffer. A sample of lipoxygenase was also subjected to three cycles of linoleate addition and HPLC separation of protein from fatty acid products. In the first cycle, two equivalents of linoleate were added. In the second and third cycles, an additional two and ten equivalents, respectively, were added to protein isolated by HPLC from the previous cycle. The EPR spectra of samples after each cycle were identical. Thus, the EPR spectrum at the top of Fig. 4 can be observed for lipoxygenase that has been through at least 14 turnovers. Spectral changes that are seen when a sample is stored for 24 h can be largely, but not completely, reversed by adding another equivalent of linoleic and reelution of the protein from HPLC in the same buffer. After a week or more, some of the signal change is irreversible by this approach but no degradation of the protein can be detected in the HPLC elution profile or in gels and activity remains unchanged. The sum of the normalized spectral intensities remains constant for at least one month, although the ratio of components changes. Other studies have shown that the EPR signal intensity gradually decreases in samples from which the fatty acid byproducts have not been removed (29). We have observed this result also with samples from which by-products of oxidation have not been removed and think the signal loss probably results from fatty acid free radicals reacting with the iron center.

The amount of the more axial component in freshly prepared ferric L-1 is a function of the length of time taken in preparing the sample. In Fig. 5, we show the low-field portion of the spectrum of a sample eluted from HPLC in phosphate buffer. Care was taken to keep the sample and HPLC column on ice during the entire procedure and to complete the procedure in 1 h. Spectral simulations, which will be described below, were employed to estimate the fraction of the signal corresponding to the more rhombic component which gives the prominent low-field signal at $g' = 7.4$: based on simulation, that fraction was 93%. Even higher levels of the rhombic species are seen in spectra of samples in which L-1 has been separated quickly from fatty acid by-products by ammonium sulfate precipitation and resuspended. The anionic composition of the sample is, of course, not well defined when ammonium sulfate pellets are resuspended.

We note briefly that large rapid-passage signals from lipoxygenase at 4 K result when the second harmonic with respect to the 100 kHz field modulation is recorded. Weger showed long ago (28) that second harmonic signals result when spins relax more completely at the ends of the modulation swings than in the middle. An example is shown in Fig. 6 where the rapid passage spectrum (Fig. 6 *a*) is compared with the result (Fig. 6 *b*) obtained by taking the numerical derivative of Fig. 6 *a*. The rapid passage signal shown for the ferric sample was about twice the intensity of the normal derivative signal recorded using the same microwave power (5 mW) and modulation amplitude (8 Gauss) that was used to record the passage signal. The derivative (Fig. 6 *b*) of the passage spectrum (Fig. 6 *a*) of the ferric L-1 sample is essentially identical to the regular derivative presentation (not shown) of the spectrum of this sample. Note in this case, that the spectrum is dominated by the near-axial component. In other cases where spectra of the more rhombic

FIGURE 7 The steps in simulating the EPR spectra for HPLC-purified ferric L-1 in 0.2 M phosphate, pH 6.8 are depicted here. Contributions to simulations of the more rhombic component (central $E/D$ of 0.065) are shown on the left. Those that contribute to the more axial component (central $E/D$ of 0.0175) are shown on the right. (*a*) The calculated absorption spectra for all of the components used in calculating the distribution in $E/D$ are shown. The spectra have not been multiplied by the gaussian weighting factors, so each spectrum shown corresponds to the same number of spins, for the various values of $E/D$, except that the vertical scale is multiplied by 2.5 for the spectra on the left, compared to those on the right. The spectra shown differ by 0.005 in the parameter $E/D$ except that two curves is omitted for clarity for the 3 to 4 transition. Significant contributions to spectra in the region shown arise from transitions between levels 1 and 2 and 3 and 4 as shown. The energy levels involved are designated by a double-headed arrow. (*b*) After applying the gaussian weighting factor to the spectra shown in *a*, the sum gives the calculated absorption spectrum shown here. (*c*) The derivative spectra corresponding to the absorption spectra shown in *b* are separated into the contributions from each significant pair of energy levels. The ripples appearing in the calculation for the 3–4 transition of the near-axial component (*right side*). (*d*) The derivative EPR spectra that are used in simulations of experimental spectra are shown. The spectra are the derivatives of those shown in *b*. All simulation parameters are given in Table 2 and axial component I was used.

and near axial species are of nearly equal amplitude, the optimum phase for detecting the second harmonic signal differs for the two signals because they saturate differently. In this case, numerical derivatives at one phase do not reproduce the first harmonic spectra. Some passage signal is exhibited by the resting ferrous enzyme as well (Fig. 6 *a*). The derivative of the passage spectrum (same conditions as those given in Fig. 6 for ferric protein) for ferrous L-1 (60 mg/ml in 0.02 M phosphate, pH 7) shows signals at $g' \sim 6$ and 4.3 and a clear manganese sextet at $g' = 2$. These species are much easier to discern by taking the derivative of a passage spectrum at high microwave power than by recording the normal EPR spectra. The occurrence of a small signal at $g' = 6$ in the spectra of the ferrous sample suggests that there may always be a portion of lipoxygenase samples in the ferric form.

## SIMULATION OF LIPOXYGENASE-1 EPR SPECTRA

Quantitative aspects of EPR spectra that extend over a wide magnetic field range, as high-spin iron spectra do, must be addressed by simulation of the spectra. One reason for this is that solution of the spin Hamiltonian gives a frequency-swept spectrum. After conversion to a field-swept spectrum, the intrinsic linewidth is no longer a constant across the spectrum (30). Thus, integration of a wide, field-swept spectrum is not a useful tool. This, and other aspects of the theory of transition metal EPR, have been discussed recently by Pilbrow (21). Lipoxygenase EPR spectra have been the subject of an earlier simulation study (17). Now, with samples of lipoxygenase that are dominated by the more rhombic component, we are able to evaluate this spectrum in more detail. The spin Hamiltonian appropriate for high-spin iron is given by Eq. 1,

$$H_S = g\beta \mathbf{B}\cdot\mathbf{S} + D(S_z^2 - \tfrac{1}{3}\mathbf{S}^2) + E(S_x^2 - S_y^2), \qquad (1)$$

where $D$ and $E$ are the axial and rhombic zero-field splitting parameters, respectively. Our computer program for spectral simulation, based on Eq. 1, includes full matrix diagonalization and has been discussed (22). Variable-frequency EPR (31) and optical spectroscopy (32) have been used to determine that the value of $D$ for lipoxygenase is greater than the X-band microwave quantum ($h\nu_{\text{X-band}} = 0.31\ \text{cm}^{-1}$, $D_{\text{lox}} \sim 1.7\ \text{cm}^{-1}$). Although perturbation theory can be used when $D$ exceeds $h\nu$ by this much, the simulations we present use the full diagonalization. Assignment of the features of the lipoxygenase spectrum can be made by noting the resonance fields of the three low-field maxima. They are at 89.0, 104.0, and 113.0 mT ($h\nu$ = 9.22 GHz). Resonances at 89.0 and 113.0 mT correspond to the low-field turning points for transitions between the lower and middle Kramers doublets of a species of $E/D = 0.065$. The peak at 104.0 mT must be that of a species with near-axial symmetry. Additional reasons for assigning this region of the spectrum to two species are that the signal at 104.0 mT is more easily saturated than the others and the relative heights of the resonances at 104.0 and 113.0 mT change as the absolute proportion of component at 104.0 mT increases (compare Figs. 4 and 5).

The features from all three principle axis directions for the more rhombic species are apparent when the partial spectrum shown in Fig. 5 is expanded in range to 400 mT. The outer width at half height of the lowest field peak (the $g_y$ feature) in the experimental spectrum is 3.2 mT in the spectrum shown in Fig. 5. This value is characteristic of L-1 in phosphate buffer. A simulation simply using this linewidth and a Gaussian lineshape gave a poor fit to the experimental spectrum in several ways. Most importantly, the width of the $g_x$ feature centered at about 147.5 mT was much narrower in the simple simulation than in the experimental spectrum (this simulation not shown in Fig. 5). Many EPR spectra of high spin iron show evidence of distributions in the parameters of the spin Hamiltonian given in Eq. 1. For high-spin ferric proteins, we (18) and others (33) have used distributions in the zero-field splitting parameters of Eq. 1 to account for the breadth and line shapes of EPR spectra. As the physical basis of the distribution cannot yet be evaluated, we use, for simplicity, a Gaussian distribution in $E$ (or in $E/D$ while $D$ is held constant) (22). Fig. 3 showed the result of a simulation which fits all regions of the more rhombic spectrum by using a single linewidth and a distribution in $E/D$ to account for the breadth of the spectral features. The parameters for the simulation are given in Table 2.

To illustrate the steps in computing the spectrum, Fig. 7 outlines the calculation. The left side of the figure shows how the more rhombic component is simulated. Steps for the more axial species are shown on the right. A selection of the components contributing to the distribution is shown in *a* as an absorption spectrum and each absorption spectrum represents the same number of spins (the Gaussian weighting function has not yet been applied). Note that there are significant contributions from transitions in the lower Kramers doublet (1–2) and the middle one (3–4) for the more rhombic species. After the spectra in *a* are weighted by a Gaussian and summed, the absorption spectra in *b* result. The derivative spectra are shown separately for transitions in each Kramers doublet in *c* and together in *d*. Finally, the more rhombic and near-axial components are added to match an experimental spectrum.

For Fig. 5, the near-axial component accounts for 7% of the spins. It is clear from Figs. 2 and 3 that the near-axial spectra have some variation with the ligands in solution with time. In choosing the parameters for the simulation shown in Fig. 5, parameters were selected that gave the feature from the more axial component at the experimentally observed $g'$-value. In fact, as the spectrum evolves with time after sample preparation, the $g'$-value

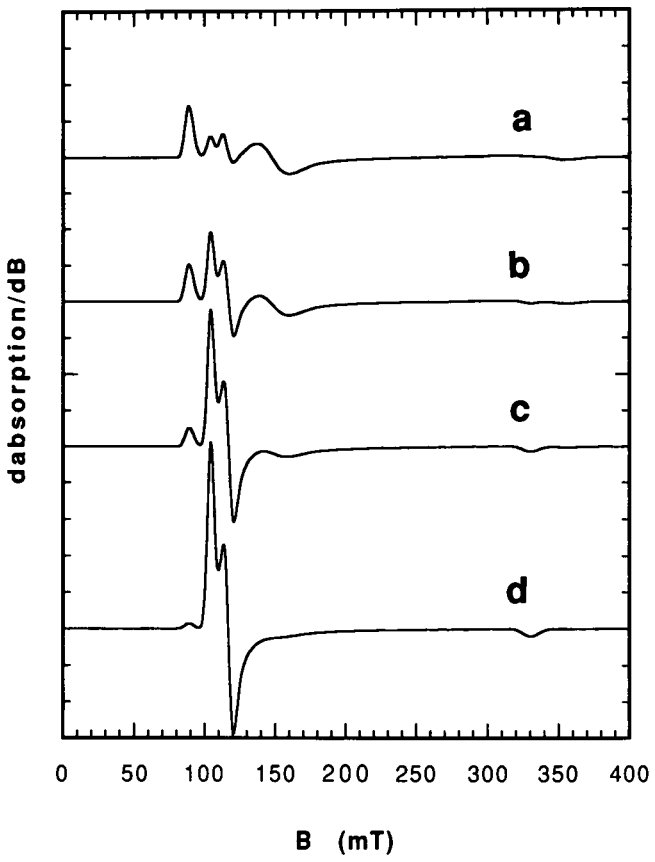


FIGURE 8 Simulations of the lipoxygenase spectra that result from different ratios of the more rhombic and the more axial species are shown. Parameters for the simulations are given in Table 2. Axial component II was used. The ratios of spins in the two species (rhombic: axial) are (*a*) (10:1), (*b*) (2:1), (*c*) (1:2), and (*d*) (1:10).

of the axial component changes slightly. Thus, we have used a second, slightly different set of parameters in some simulations of the more axial component. The simulation shown in Fig. 2, superimposed on the experimental spectrum of the sample to which glycerol had been added, used the parameters of "axial component II" given in Table 2. The simulation of the more rhombic component and of axial component II have been added in different proportions and the results are shown in Fig. 8 for the spectral range from 0 to 400 mT. The same number of spins is represented by each spectrum as shown. The parameters used for Fig. 8 give good fits to samples in phosphate buffer. Although we have used a very different simulation approach from that of Slappendel et al. (17), our result in Fig. 8 *b* for the 1:1 mixture is quite similar to theirs.

Simulations have been applied to make a quantitative analysis of the ferric iron formed as lipoxygenase is titrated with hydroperoxide. This is a complicated reaction to analyse by EPR because the chemistry is irreversible and the fatty acid product of the reaction may undergo secondary reactions so that there can be more than one fatty acid species interacting with the iron center. Although the ratio of more rhombic to near axial species decreases as increasing amounts of hydroperoxide are added to the enzyme, the total ferric iron represented by the EPR signals should be more simply related to the ratio of hydroperoxide to enzyme. The simulations in Fig. 8 yield normalization constants for converting signal intensity to relative amount of ferric iron. When the more rhombic and near axial spectra correspond to equal amounts of iron in each site, the relative peak heights for the maxima at 89, 104, and 113 mT in simulated spectra are 0.46, 1.71, and 1.0. Using these figures to convert peak heights into amounts of ferric iron contributing to the spectrum, the titration curve shown in Fig. 9 results. The figure legend notes that the points in Fig. 9 were obtained for samples with absolute lipoxygenase concentrations from 0.26 to 0.53 mM. Straight lines connect the points for clarity. No model was chosen to fit the points because this reaction is irreversible. This titration was carried out at pH 6.4. The reported purple color and $g' = 4.3$ signal (36) were not seen in any of the samples, including the one with excess hydroperoxide, used for Fig. 8. We do see the reported optical and EPR spectra when more than one equivalent of hydroperoxide is added at pH 9.

## DISCUSSION

This work differs from an earlier report (16) of the factors affecting the lineshape of L-1 EPR spectra in the extent of the more rhombic component obtained. The differences in the experimental conditions for that report and this one provide insight into the origin of the spectral variability for EPR of L-1. When the anionic composition of the buffer is controlled, by HPLC purification,

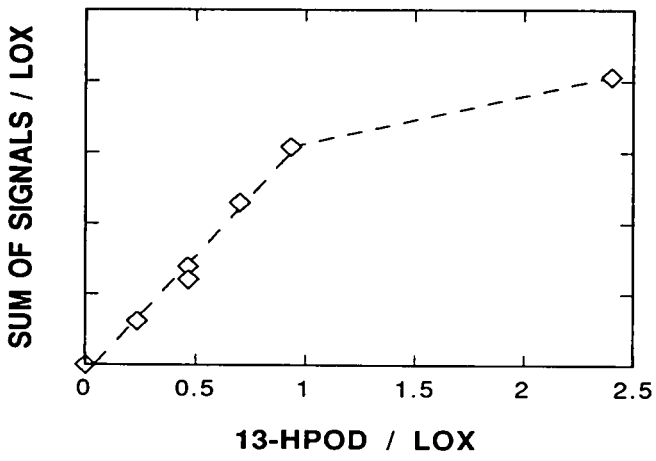


FIGURE 9 Titration at pH 6.4 (citrate/phosphate, 0.2 M phosphate) of lipoxygenase (LOX) with 13-HPOD gives multicomponent EPR signals. The simulations of Fig. 8 were used to normalize signal amplitudes on a per iron basis. The sum of signals shown represents the total ferric iron/protein. At 13-HPOD/LOX molar ratios of 0.234, 0.466, 0.468, 0.702, 0.936, and 2.40, the lipoxygenase concentrations used were 0.53, 0.49, 0.26, 0.46, 0.43, and 0.29, respectively.

the EPR spectra of L-1 are found to depend more on the nature of the anion than on pH. Comparisons of the EPR spectra when L-1 is isolated in formate or phosphate buffers illustrate this point. Samples prepared at pH's from 6.8 to 7.8 in 0.2 M buffers of either composition give EPR spectra in which the lowest field feature is at $g' = 7.4$ when the buffer is phosphate and at $g' = 7.45$ when it is formate. A large number of ligands are now known, from the studies reported here and from earlier work by others (16, 32), to influence the EPR spectra of lipoxygenase. Although the components contributing to the spectra fall generally into the group described by "near-axial" or "more rhombic", within each of these spectral categories there are small differences that depend on the nature of the ligands available. Also, azide is an exception in that it is the only ligand listed that gives a spectrum characteristic of near rhombic symmetry (Fig. 3). Table 1 summarizes data on the EPR spectra of L-1 in the presence of ligands. There is not a clear distinction between the EPR lineshapes resulting from neutral and anionic ligands. For example, cyanide (16) and imidazole favor axial signals while pyridine and phosphate favor the more rhombic signals. There may be both specific and non-specific effects on the EPR spectra. For the specific effects, the following general equilibrium expression 2 probably has a different equilibrium constant for each ligand ($L$).

$$(L-1)\text{-}X + L = (L-1)\text{-}L + X. \qquad (2)$$

Affinity of charged ligands for the iron center may provide a mechanism for charge compensation as the iron center alternates between ferric and ferrous in the catalytic cycle. The species designated "$X$" in Eq. 2 could be an open coordination site or a displaceable ligand. Alcohols have weak affinities for the iron center in lipoxygenase with binding constants from 3 to 260 mM (34). The spectra shown in Fig. 1 suggest that buffer anions also may have affinities on the order of 100 mM for freshly oxidized lipoxygenase. Alternatively, since the more rhombic species is kinetically unstable, it is possible that ligands favoring the near axial species simply accelerate the rate of structural rearrangement to a structure that is more stable when the iron center is ferric. Since changes in symmetry at iron are partially reversible at early times but not at later ones, there must be more than one step involved in the changes that result in altered EPR spectra. General ionic strength effects may also be important in influencing conformational states of lipoxygenase: although we find no differences large enough, between samples in 0.02 and 0.2 M buffers, to be detected in CD spectra, there is a small effect of ionic strength on activity assays (37). The effects reported here suggest that each step in the complex lipoxygenase kinetic pathway (11) should be examined as a function of potential metal ligands, their concentrations and pH. Other examples of metalloenzymes that have multiple EPR spectra arising from interaction of the metal with buffer ligands are the molybdenum-containing hydroxylases (35).

The symmetry of the more-rhombic component of the lipoxygenase iron center ($E/D = 0.065$) is such that transitions in both the lower and middle Kramers doublets should be seen. The transition in the middle doublet for this symmetry may not have been noticed before because it is at nearly the same resonance field as the $g_y$ component of the more axial spectrum. As shown in Fig. 7 *a*, the low-field turning point for the 3–4 transition is almost invariant for quite a range of $E/D$ values. It should be apparent as a peak in samples for which $E/D > 0.05$. In fact, we are now able to assign a small shoulder at $\sim$110 mT in the spectra of phenylalanine hydroxylase (25, 18) to a middle doublet transition.

This article is dedicated to Professor Harden M. McConnell who has provided years of inspiration.

It is a pleasure to acknowledge the help of Z. V. Mavrophilipos, D. M. Lang, H. Q. Wu, and A. C. Colom with some of the protein preparations and in repeating some of the experiments. We are grateful to the National Institutes of Health for support of this work under grant number GM36232.

*Received for publication 24 September and in final form 23 November 1992.*

## REFERENCES

1. Gardner, H. W. 1991. Recent investigations into the lipoxygenase pathway of plants. *Biochim. Biophys. Acta.* 1084:221–239.
2. Bryant, R. W., J. M. Bailey, T. Schewe, and S. M. Rapoport. 1982. Positional specificity of a reticulocyte lipoxygenase. *J. Biol. Chem.* 257:6050–6055.
3. Crooke, S. T., and A. Wong, editors. 1991. Lipoxygenases and their Products. Academic Press, San Diego. 300 pp.
4. Ylä-Herttuala, S., M. E. Rosenfeld, S. Parthasarathy, C. K. Glass, E. Sigal, J. L. Witztum, and D. Steinberg. 1990. Colocalization of 15-lipoxygenase mRNA and protein with epitopes of oxidized low density lipoprotein in macrophage-rich areas of atherosclerotic lesions. *Proc. Natl. Acad. Sci. USA.* 87:6959–6963.
5. Derian, C. K., and D. F. Lewis. 1992. Activation of 15-lipoxygenase by low density lipoprotein in vascular endothelial cells. relationship to the oxidative modification of low density lipoprotein. *Prostaglandins, Leukotrienes and Essential Fatty Acids.* 45:49–57.
6. Van der Zee, J., T. E. Eling, and R. P. Mason. 1989. Formation of free radical metabolites in the reaction between soybean lipoxygenase and its inhibitors. An ESR study. *Biochemistry.* 28:8363–8367.
7. Stallings, W. C., B. A. Kroa, R. T. Carroll, A. L. Metzger, and M. O. Funk. 1990. Crystallization and preliminary x-ray characterization of a soybean seed lipoxygenase. *J. Mol. Biol.* 211:685–687.
8. Steczko, J., C. R. Muchmore, J. L. Smith, and B. Axelrod. 1990. Crystallization and preliminary x-ray investigation of lipoxygenase-1 from soybeans. *J. Biol. Chem.* 265:11352–11354.
9. Boyington, J. C., B. J. Gaffney, and L. M. Amzel. 1990. Crystallization and preliminary x-ray analysis of soybean lipoxygenase-1, a non-heme iron-containing dioxygenase. *J. Biol. Chem.* 265:12771–12773.

10. Sloane, D. L., M. F. Browner, Z. Dauter, K. Wilson, R. J. Fletterick, and E. Sigal. 1990. Purification and crystallization of 15-lipoxygenase from rabbit reticulocytes. *Biochem. Biophys. Res. Commun.* 173:507–513.

11. Schilstra, M. J., G. A. Veldink, J. Verhagen, and J. F. G. Vliegenthart. 1992. Effect of lipid hydroperoxide on lipoxygenase kinetics. *Biochemistry.* 31:7692–7699.

12. Pistorius, E. K., and B. Axelrod. 1974. Iron, an essential component of lipoxygenase. *J. Biol. Chem.* 249:3183–3186.

13. de Groot, J. J. M. C., G. A. Veldink, J. F. G. Vliegenthart, J. Boldingh, R. Wever, and B. F. van Gelder. 1975. Demonstration by EPR spectroscopy of the functional role of iron in soybean lipoxygenase-1. *Biochim. Biophys. Acta.* 377:71–79.

14. Pistorius, E. K., B. Axelrod, and G. Palmer. 1976. Evidence for participation of iron in lipoxygenase reaction from optical and electron spin resonance studies. *J. Biol. Chem.* 251:7144–7148.

15. Mulliez, E., J.-P. Leblanc, J.-J. Girerd, M. Rigaud, and J.-C. Chottard. 1987. 5-Lipoxygenase from potato tubers. Improved purification and physicochemical characteristics. *Biochim. Biophys. Acta.* 916:13–23.

16. Slappendel, S., R. Aasa, B. G. Malmström, J. Verhagen, G. A. Veldink, and J. F. G. Vliegenthart. 1982. Factors affecting the line-shape of the EPR signal of high-spin Fe(III) in soybean lipoxygenase-1. *Biochim. Biophys. Acta.* 708:259–265.

17. Slappendel, S., G. A. Veldink, J. F. G. Vliegenthart, R. Aasa, and B. G. Malmström. 1981. EPR spectroscopy of soybean lipoxygenase-1: description and quantification of the high-spin Fe(III) signals. *Biochim. Biophys. Acta.* 667:77–86.

18. Yang, A. S., and B. J. Gaffney. 1987. Determination of relative spin concentration in some high-spin ferric proteins using E/D-distribution in electron paramagnetic resonance simulations. *Biophys. J.* 51:55–67.

19. Fee, J. A., G. J. McClune, A. C. Lees, R. Zidovetzki, and I. Pecht. 1981. The pH dependence of the spectral and anion binding properties of iron containing superoxide dismutase from *E. coli* B: an explanation for the azide inhibition of dismutase activity. *Israel J. Chem.* 21:54–58.

20. Blum, H., B. Chance, and W. J. Litchfield. 1978. Effect of pH on bovine liver catalase as determined by electron paramagnetic resonance. *Biochim. Biophys. Acta.* 534:317–321.

21. Pilbrow, J. R. 1990. Transition Ion Electron Paramagnetic Resonance. Clarendon Press, Oxford. 717 pp.

22. Gaffney, B. J., and H. J. Silverstone. Simulation of the EMR spectra of high spin iron in proteins. *In* Biological Magnetic Resonance, EMR of Paramagnetic Molecules. L. J. Berliner and J. Reuben, editors. Plenum Press, New York.

23. Axelrod, B., T. M. Cheesbrough, and S. Laakso. 1981. Lipoxygenase from soybeans. *Methods Enzymol.* 71:441–451.

24. Kemal, C., P. Louis-Flamberg, R. Krupinski-Olsen, and A. L. Shorter. 1987. Reductive inactivation of soybean lipoxygenase 1 by catechols: a possible mechanism for regulation of lipoxygenase activity. *Biochemistry.* 26:7064–7072.

25. Bloom, L. M., S. J. Benkovic, and B. J. Gaffney. 1986. Characterization of phenylalanine hydroxylase. *Biochemistry.* 25:4204–4210.

26. Spaapen, L. J. M., G. A. Veldink, T. J. Liefkens, J. F. G. Vliegenthart, and C. M. Kay. 1979. Circular dichroism of lipoxygenase-1 from soybeans. *Biochim. Biophys. Acta.* 574:301–311.

27. Ramadoss, C. S., and B. Axelrod. 1982. High-performance liquid chromatographic separation of lipoxygenase isozymes in crude soybean extracts. *Analyt. Biochem.* 127:25–31.

28. Weger, M. 1960. Passage effects in paramagnetic resonance experiments. *Bell System Tech. J.* 39:1013–1112.

29. Slappendel, S., B. G. Malmström, L. Petersson, A. Ehrenberg, G. A. Veldink, and F. G. Vliegenthart. 1982. On the spin and valence state of iron in native soybean lipoxygenase-1. *Biochem. Biophys. Res. Commun.* 108:673–677.

30. Aasa, R., and T. Vänngård. 1975. EPR signal intensity and powder shapes: a reexamination. *J. Magn. Res.* 19:308–315.

31. Slappendel, S., G. A. Veldink, J. F. G. Vliegenthart, R. Aasa, and B. G. Malmström. 1980. EPR spectroscopy of soybean lipoxygenase-1; determination of the zero-field splitting constants of high-spin Fe(III) signals from temperature and microwave frequency dependence. *Biochim. Biophys. Acta.* 642:30–39.

32. Zhang, Y., M. S. Gebbhard, and E. I. Solomon. 1991. Spectroscopic studies of the non-heme ferric active site in soybean lipoxygenase. Magnetic circular dichroism as a probe of electronic and geometric structure. Ligand-field origin of zero-field splitting. *J. Am. Chem. Soc.* 113:5162–5175.

33. Fiamingo, F. G., A. S. Brill, D. A. Hampton, and R. Thorkildsen. 1989. Energy distributions at the high-spin ferric sites in myoglobin crystals. *Biophys. J.* 55:67–77.

34. Slappendel, S., R. Aasa, K.-E. Falk, B. G. Malmström, T. Vänngard, G. A. Veldink, and J. F. G. Vliegenthart. 1982. $^1$H-NMR spectroscopic study on the binding of alcohols to soybean lipoxygenase-1. *Biochim. Biophys. Acta.* 708:266–271.

35. Hille, R., and V. Massey. 1985. Molybdenum-containing hydroxylases: xanthine oxidase, aldehyde oxidase and sulfite reductase. *In* Molybdenum Enzymes. T. G. Spiro, editor. Wiley-Interscience, New York. 443–518.

36. Slappendel, S., G. A. Veldink, J. F. G. Vliegenthart, R. Aasa, and B. G. Malmström. 1983. A quantitative optical and EPR study on the interaction between Soybean Lipoxygenase-1 and 13-hydroperoxylinoleic Acid. *Biochim. Biophys. Acta.* 747:32–36.

37. Christopher, J., E. Pistorius, and B. Axelrod. 1970. Isolation of an isozyme of soybean lipoxygenase. *Biochim. Biophys. Acta.* 198:12–19.